Appl. Phys. B 50, 221–226 (1990)

Applied Physics B Photophysics and Laser Chemistry

Multiphoton Ionization Studies of Amines with UV-VIS Lasers

Gary Siuzdak and Joseph J. BelBruno

Department of Chemistry, Dartmouth College, Hanover, NH 03755, USA

Received 8 September 1989/Accepted 15 November 1989

Abstract. Three and four photon ionization studies at 355 and 532 nm are presented for the isomeric propylamines and *n*-pentylamine. Ionic fragmentation patterns and ion yields are presented as a function of laser wavelength and fluence. These time-of-flight (TOF) mass spectra are compared with both electron impact data and the TOF mass spectra of the previously reported butylamines. A brief discussion of the dynamics of the decomposition process is presented in light of the butylamine results and competitive ionic fragmentation pathways.

PACS: 33.80K

Multiphoton ionization (MPI) and multiphoton ionization mass spectrometry (MPI-MS) have been employed [1] in recent years to great advantage in the study of the mass fragmentation of fragile molecules [2] as well as in the observation of photoinitiated chemical dynamics [3]. The technique has been especially valuable in those instances where electron impact mass spectrometry leads to extensive and somewhat indiscriminate fragmentation of the parent molecule.

We have recently employed MPI-MS in the study of the chemical dynamics of the isomerization of alkylamine radical cations [4]. For butylamine ions, it was shown that the less branched amines undergo very rapid rearrangement, while sec- and tert-butylamine radical cations are stable to isomerization. In this paper, we report on the MPI-MS studies of both higher and lower alkylamines. In particular, the mass spectral fragmentation patterns of the propylamines and *n*-pentylamine are presented and discussed in terms of the butylamine data and the mechanism of parent radical cation fragmentation. A skeletal size threshold for isomerization and novel competitive kinetic pathways have been detected.

The ions were created with laser radiation of both visible and UV frequencies using a linear time-of-flight mass spectrometric technique. In the following sections, the ionic fragmentation patterns are presented as a function of laser frequency and fluence. The data are compared with the electron impact mass spectra and a previously developed model for the fragmentation mechanism of the parent cation.

1. Experimental

The experiments described in this report were performed with a linear time-of-flight mass spectrometer of the Wiley-McLaren design. A schematic diagram is shown in Fig. 1. The apparatus consisted of two independently pumped chambers, the source and drift tube regions, separated by an aperture. The oil diffusion-mechanical roughing pump combination for either chamber was capable of reducing the pressure to approximately 10^{-6} Torr in the absence of any sample flow. The source region consisted of a repelling plate and a pair of accelerating grids with the repelling plate and grid assembly separated by 0.85 cm and the accelerating grids spaced 2.64 cm apart. Potentials of up to 3 kV could be applied to any two of the three plates, but for most of the reported work, only the repelling plate was employed with an applied potential of 2 kV. The sample was admitted to the source region via a molecular leak from a reservoir pressure of ~50–200 Torr. The pressure in the source region, as measured by a cold cathode gauge, was always less than $\sim 8 \times 10^{-5}$ Torr, resulting in an estimated minimum mean free path in that chamber of 0.25 m. The drift tube was 105 cm in length and the pressure in this

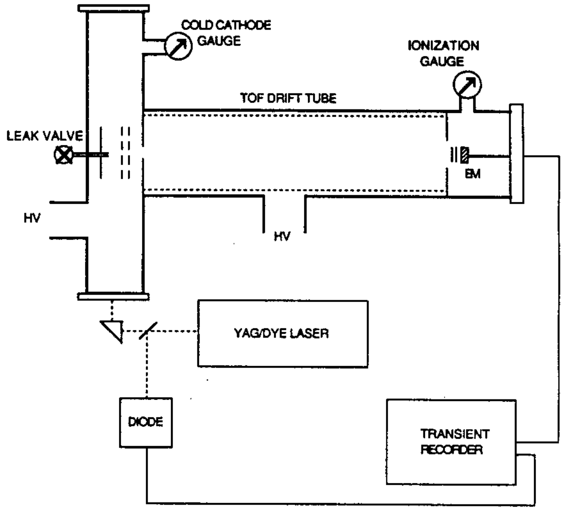

Fig. 1. Schematic diagram of the time-of-flight apparatus. Details are presented in the text

region was maintained in the 10^{-6} Torr range at all times. Ions were detected by means of a Galileo electron multiplier optimized for fast pulsed operation. The ion time arrival spectrum was sent directly to a transient recorder for signal averaging and manipulation. The time resolution of this device is 10 ns and all reported traces are the average of 128 laser pulses. The ion arrival time spectra are converted to mass spectra by calibration using a mixture of chlorofluoro- and bromochlorofluorocarbons and a computer analysis of the arrival times of the halogen atoms. The resolution of the detector was 1 amu throughout the spectrum of the halocarbons ($m/z > 110$).

Laser multiphoton mass spectra (total charge vs. amu) were obtained at two different wavelengths. Radiation at 532 nm (2.4 eV photon energy) and 355 nm (3.5 eV photon energy) was produced by frequency doubling and tripling of the fundamental output of a Nd:YAG laser (Spectra Physics DCR-11, 6 ns pulsewidth). Radiation at both of these wavelengths was focused into the source region by means of a 15 cm focal length lens. Pulse energies for the harmonics of the Nd:YAG laser ranged from 0.5 to 25 mJ per pulse, with the high end limited by filters or controlling the Q-switch delay of the laser. The laser energies were measured at the input window of the time-of-flight apparatus.

At both wavelengths, irradiation of the propylamines and the pentylamine readily produced ions. The ionization potentials of the propylamines are 8.78 and 8.72 eV, respectively for the *n*- and iso-compounds, so that depending upon the wavelength chosen for a particular experiment, 3 or 4 photon ionization of the parent molecule was expected [5]. The ionization potential of the *n*-pentylamine has not been definitely reported, but based upon the average butylamine and propylamine ionization limits, it is expected to be in the range from 8.7–8.9 eV. Resonant enhancement of the ionization process could occur for all amines through the $n \rightarrow 3s$ Rydberg transition, which has previously been reported only for the butylamines and the lower alkylamines.

Samples of the propylamines were purchased from Aldrich as greater than 99% purity, but were further distilled and stored under vacuum in glass sample bulls prior to use. The purity of the redistilled material was confirmed by GC/MS, NMR and IR techniques and no discernible impurities were discovered. The *n*-pentylamine was purchased from Fluka Chemicals. Samples of the ND_2 amines were prepared by stirring the amines in D_2O overnight. Analysis by the same techniques cited above indicated greater than 99% conversion to R-ND_2.

2. Results

The electron impact (EI) mass fragmentation patterns for the target molecules are well-known [6]. These spectra are shown in Fig. 2, so that comparison may be made with the MPI data. For *n*-propylamine, the most intense feature occurs at m/z 30 and corresponds to an apparent α-cleavage of the parent radical cation to a fragment with the empirical formula $CH_4\dot{N}^+$. Very small yields of parent ion and C_2 fragment ions ($m/z \sim 40$) are also observed. The iso-propylamine EI fragmentation pattern follows analogously. The major feature occurs at m/z 44 and again may be ascribed to an apparent α-cleavage of the parent ion to produce a $C_2H_6N^+$ fragment. Small quantities of lower m/z fragments and parent ion are also detected. Finally, the *n*-pentylamine EI mass spectrum is also dominated by a process that corresponds to α-cleavage to produce the m/z 30 fragment as observed in *n*-propylamine. Very small yields of parent ion and *larger* fragments are also observed and are attributed to molecular rearrangements prior to fragmentation or higher order C–C bond cleavage.

The MPI mass fragmentation patterns for *n*-propylamine are shown in Fig. 3 as a function of laser intensity. At low laser intensities ($\sim 10^7$ W cm^{-2}) the only observed fragment is m/z 30 in agreement with the EI mass spectrum. The implication is that the same pathway observed for 70 eV electron impact may also be effected optically. As the laser intensity is increased to 10^9 W cm^{-2}, more extensive fragmentation of the molecule is observed. This is consistent with the usual observations in comparing EI and MPI fragmentation. Interestingly, a larger quantity of the M^+–H ion is produced at the higher energy. The total ion yield

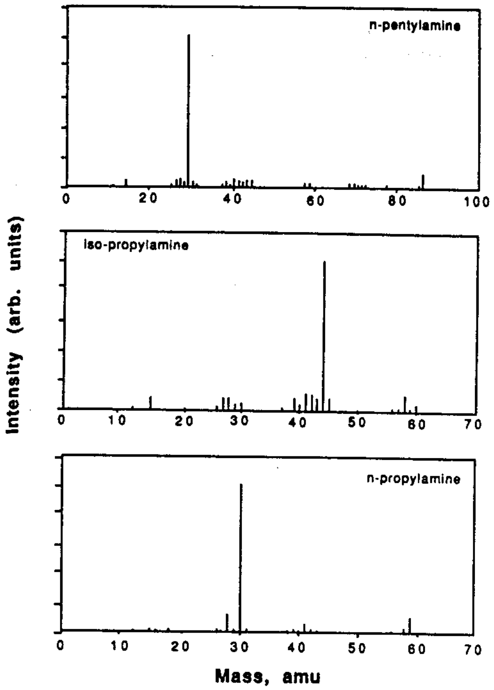

Fig. 2. Electron impact mass fragmentation patterns. The numerical data for this figure were obtained from [6]

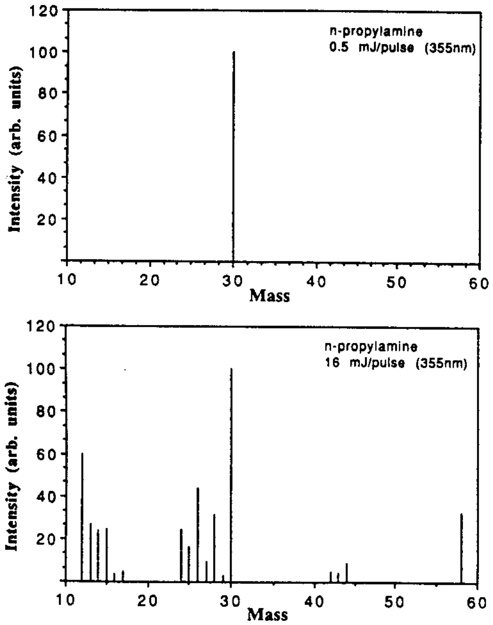

Fig. 3. Multiphoton mass fragmentation patterns for *n*-propylamine with 355 nm laser excitation

increases by ~two orders of magnitude over the change in laser intensity. Note that the two mass spectra shown in the figure have been separately normalized so that the base peak of each is 100. It appears that only a very small quantity of C_2 fragments is produced. The ratio of the fragments *m/z* 30 to *m/z* 44 is nearly identical to that recorded in the EI spectrum shown in Fig. 2.

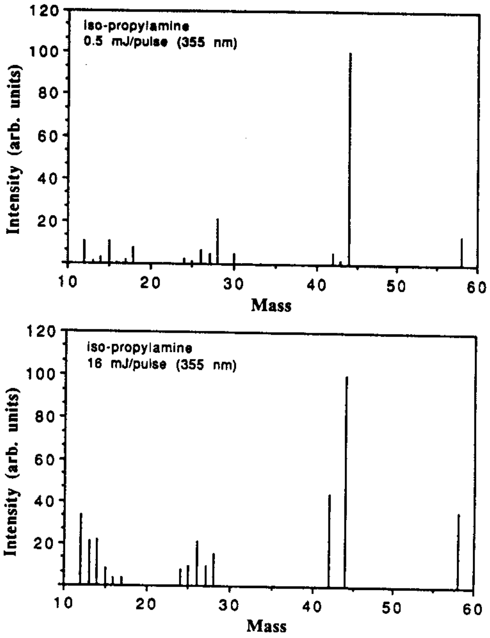

Fig. 4. Multiphoton mass fragmentation patterns for iso-propylamine with 355 nm laser excitation

In Fig. 4, the MPI fragmentation pattern for iso-propylamine is shown at the same laser energies used for the results presented in Fig. 3. The spectra are analogous to those already shown for *n*-propylamine. That is, the MPI spectrum at low energy resembles that obtained from electron impact, the total ion yield increases dramatically with laser energy and the fragmentation becomes more extensive at higher laser energies. Again, molecular rearrangements prior to fragmentation appear to be minimal. Again, a distinguishing feature of the MPI spectra is the presence of hydrogen atom loss channels which do not appear to be readily available to the electron impact produced parent ion. This effect is characterized most dramatically by the *m/z* 42 and *m/z* 58 fragments present in the higher energy spectrum shown in Fig. 4.

Figure 5 contains propylamine MPI fragmentation spectra for excitation at 532 nm. The lower photon energy increases the order of the ionization process and a greater laser intensity is required to obtain a signal. As a result, only data acquired for a laser intensity of $\sim 2 \times 10^9$ W cm^{-2} is presented. These spectra are strikingly similar to those recorded at 355 nm. In this particular instance, the frequency dependent nature of the MPI fragmentation is lost.

Finally, Fig. 6 presents the MPI data for the *n*-pentylamine molecule. Comparison of these spectra

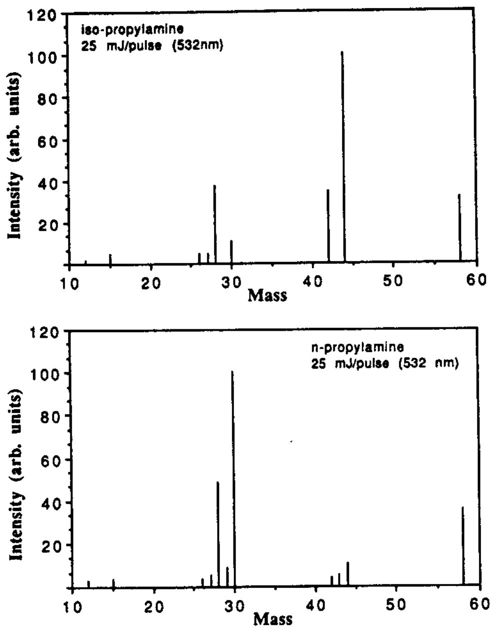

Fig. 5. Multiphoton mass fragmentation patterns for *n*-propylamine and iso-propylamine with 532 nm laser excitation

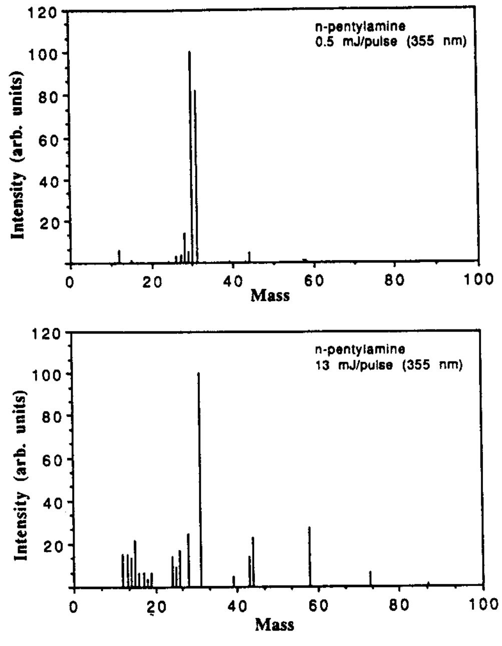

Fig. 6. Multiphoton mass fragmentation patterns for *n*-pentylamine with 355 nm laser excitation

with those contained in Fig. 2 for EI indicates that MPI and electron impact ionization are nearly identical at low laser intensities, but that at higher laser intensities the larger fragment ions are produced in much higher yields by MPI than by means of EI. In particular, the m/z 58 fragment is characteristic of butylamine fragmentation as are those at m/z 43 and 44. A butylamine-derived ion, M^+–H, is also observed at m/z 58. We note in passing that H-atom loss channels again seems to be more prevalent with the MPI technique.

The dependence of the total ion yield, as well as that of many of the fragment ion yields, has been studied for the propylamines. By means of the usual log-log plots of ion yield vs. laser power, the total ion yield, and that of most fragments, was observed to depend upon a fractional order of the laser power for 355 nm excitation. The ion yield is easily saturated. Fragment ions were found by thermodynamic considerations to require 8 or more photons at this wavelength [7]. The fact that the fragments show a much weaker laser power dependence than is thermodynamically required is indicative of a saturated ladder-switching mechanism. The absorption of the laser energy by the parent ion and any fragment ion is sufficiently rapid such that the total ion yield depends only on the kinetics of formation of the parent ion [8]. The assignment of the fragments to empirical structures containing – NH_2 was confirmed by means of D_2 amines.

3. Discussion

The MPI mass spectra, especially at the higher laser powers, exhibit considerably more extensive fragmentation than the EI spectra. This is typically observed in MPI-MS and is attributed to very efficient ladder-switching. That is, once the threshold for parent ion formation is attained, the ion is formed and subsequent laser absorption occurs in the ion manifold. Once an energy threshold for fragmentation in an ion manifold is reached, that fragmentation occurs and the fragments may then absorb additional photons. In the current work, it appears that the absorption by the cations is sufficiently rapid so as to be saturated.

In contrast to most MPI studies [9], the EI and MPI fragmentation patterns show many similarities, especially for the propylamines. In comparison, an MPI [4] study of the isomeric butylamines indicated that rearrangement processes were very rapid for the lesser branched primary amines. On the other hand, the *n*-pentylamine results shown in Fig. 6 also indicate that rapid (within the 6 ns laser pulse) isomerization and rearrangement mechanisms may effectively compete with, and even dominate, direct fragmentation. One very plausible explanation for this contrast in kinetic behavior is the fact many fewer low frequency vibrational modes are available for the propylamines as compared with the larger alkylamines. The availability of such low frequency sinks for the excess excitation energy was shown to be a critical factor in the opening of *isomerization* channels in the butylamine cations. For example, sec-butylamine cation was observed to be stable to isomerization, which was shown by RRKM calculations to be a slower decomposition pathway than fragmentation at lower photon energies. For this particular butylamine, the cross-over point [3] was calculated to be well above the energy of the available laser photons. On the other hand, iso- and *n*-butylamine cations were found to readily undergo isomerization to more stable forms even at lower laser frequencies. It appears that the three carbon chain is simply below the threshold for the accessibility of isomerization pathways.

Previous studies [10, 11] have reported contradictory conclusions with regard to the skeletal onset of H- and NH_3^+-rearrangements, currently believed to be the mechanistic pathways leading to extensive, non-α-cleavage fragmentation in larger alkylamine radical cations. However, all reports agree in the observation that such rearrangements do not occur in C_3 amines and for ionization/fragmentation via high energy electron impact. Rearrangement processes have been postulated to proceed through cyclic transition states [10] that are thermodynamically unstable for C_3, and perhaps C_4, amines. One expects; therefore, that the propylamines should fragment by α-cleavage with little or no contribution from competing pathways. The presence of the rearrangement channels may be best confirmed by the observation of H/D scrambling in fragmentation of the ND_2 samples. No such scrambling was observed for the propylamines, confirming the direct nature of the fragmentation process.

The results involving the *n*-pentylamine mass spectrum are an interesting corroboration of this interpretation. The mass fragmentation pattern appears to indicate that aside from the expected α-cleavage, a significant number of the radical cations undergo γ-cleavage to produce the *n*-butylamine cation. Comparison of the *m/z* 35–75 portion of the data in Fig. 6 to the reported MPI results for *n*-butylamine indicates a considerable number of matching fragment ratios, confirming the nature of at least one of the additional decomposition channels for the C_5 cation. Deuterated *n*-pentylamine was not analyzed; however, the participation of rearrangement channels was inferred by the wealth of non-α-cleavage fragmentation. At least one of the *n*-pentylamine fragments may be a result of the H/NH_3^+ rearrangement [10, 11]. This process has been shown to produce *m/z* 44 fragments in abundance and such fragments are present at the 20% level in Fig. 6.

The greater probability of the *m/z* 58 fragment ion for the propylamines at higher laser intensities is an intriguing and, initially, a counterintuitive result. One does not expect large fragments to increase in yield in this manner. However, this fragment lies ~1 eV above that resulting from C–C bond fission (in the parent ion) [8]. Therefore, absorption of an additional photon is required for creation of this product. Absorption of that photon is in competition with bond cleavage in the parent ion and the rates become comparable only at the higher laser intensities. This type of kinetic behavior has not been previously reported.

One interesting aspect of this research is the lack of any wavelength specificity. Earlier research in our group [4] and others [12] has indicated that the lowest electronic transition corresponds to an $n \rightarrow 3s$ Rydberg excitation ($X \rightarrow A$) with an origin at approximately 42,000 cm^{-1}, depending upon the particular chain length of the alkylamine. The higher excited states have been relatively unexplored. Two photons at 355 nm and three photons at 532 nm would be required to attain an energy greater than the vibrationless ground state of the 3*s* level. Both of these excitation schemes would result in approximately 56,000 cm^{-1} of energy input. In any event, production of the molecular ion via either wavelength would result in an ion with excess energy and a high probability for fragmentation. In addition, one must conclude from the similarity of the mass spectra, that the ions involved in ladder-switching mechanism readily absorb either wavelength.

In conclusion, the results presented above appear to indicate that there are skeletal constraints on the available decomposition channels for the unimolecular reactions of alkylamine cations. Moreover, we have observed a novel kinetic competition in the radical cation electronic manifold. It would be useful to pursue theoretical aspects of these results, especially with regard to electronic structure calculations and kinetic modeling. Such work is now underway.

Acknowledgement. This research was partially supported by the National Science Foundation through Grant No. CHE-85-21664 (J.J.B.).

4. References

1. See, for example (a) D.H. Parker: In *Ultrasensitive Laser Spectroscopy*, ed. by D.S. Kliger (Academic, New York 1983) p. 233–309; (b) U. Boesl, H.J. Neusser, E.W. Schlag: Z. Naturforsch. **33** A, 1546 (1978); (c) S. Rockwood, J.P. Reilly, K. Hohla, K.L. Kompa: Opt. Commun. **28**, 175 (1979)
2. For a review see J. Grotemeyer, E.W. Schlag: Angew. Chem. Int. Ed. Engl. **27**, 447 (1988). A description of the technique may be found in: R.C. Beavis, J. Lindner, J. Grotemeyer, E.W. Schlag: Chem. Phys. Lett. **146**, 310 (1988)
3. (a) D.H. Parker, R.B. Bernstein: J. Phys. Chem **86**, 60 (1982); (b) H. Kühlewind, H.J. Neusser, E.W. Schlag: J. Phys. Chem. **89**, 5600 (1985)
4. G. Siuzdak, J.J. BelBruno: J. Phys. Chem. (to be published)

5. K. Watanabe, T. Nakayama, J. Mottl: J. Quant. Spectrosc. Radiat. Transfer **29**, 216 (1969)
6. E. Stenhagen, S. Abrahamsson, F.W. McLafferty: *Atlas of Mass Spectral Data* (Wiley, New York 1969)
7. (a) K.W. Egger, A.T. Cocks: Helv. Chim. Acta **56**, 1516 (1973); (b) F.T. Wall: *Chemical Thermodynamics* (W.H. Freeman, San Francisco 1974); (c) F.H. Field, J.L. Franklin: *Electron Impact Phenomena* (Academic, New York 1970)
8. R.B. Bernstein: J. Phys. Chem. **86**, 1178 (1982)
9. R. Bruzzese, I. Rendina, A. Sasso, E. Borsella: Appl. Phys. B **44**, 45 (1987)
10. (a) H.E. Audier, J.P. Denhez, A. Milliet, G. Sozzi: Can. J. Chem. **62**, 931 (1984); (b) H.E. Audier, J.C. Tabet: Org. Mass Spectrom. **20**, 313 (1985)
11. (a) S. Hammerum: Tetrahedron Lett. **22**, 157 (1981); (b) H.E. Audier, A. Milliet, J.P. Denhez: Org. Mass Spectrom. **18**, 131 (1983); (c) S. Hammerum, S. Ingemann, N.M.M. Nibbering: Org. Mass Spectrom. **20**, 314 (1985)
12. (a) M. Tsuboi, A.Y. Kirakawa, H. Kawashima: J. Mol. Spectrosc. **29**, 216 (1969); (b) A.Y. Hirakawa, H. Miyazaki, M. Tsuboi: Bull. Chem. Soc. Japan **45**, 757 (1972)